

# A Simple Orthomode Transducer for Centimeter to Submillimeter Wavelengths

A. Dunning, S. Srikanth, and A. R. Kerr

**Abstract** – We describe a simple orthomode transducer suitable for operation from centimeter to submillimeter wavelengths with appropriate scaling. It is fabricated as a split-block assembly with all waveguides in the same plane, and requires no septum or polarizing wires. The OMT operates over a 1.3:1 frequency band, narrower than a full waveguide band (typically 1.5:1). For a WR-10 version of the OMT, covering 78-102 GHz, the polarization isolation is  $> 37$  dB and the return loss at the rectangular waveguide ports  $> 24$  dB. The practical upper frequency for this design is probably limited by the precision of alignment that can be achieved between the block halves, which affects the polarization isolation.

**Index Terms** — Orthomode transducers, waveguide junctions, multimode waveguides, millimeter wave circuits.

## I. INTRODUCTION

In designing broadband orthomode transducers (OMTs) it is desirable to maintain symmetry about both input polarizations to prevent generation of higher-order modes. However, most schemes which have been devised to accommodate these symmetry conditions [1][2][3][4][5][6] result in considerable complexity compared with designs which are symmetrical about only one plane. At submillimeter wavelengths this extra complexity presents an additional obstacle to fabrication. We describe an OMT symmetrical about only one plane which can be fabricated as a simple split block assembly and which requires no polarizing wires or septum.

For an OMT with a square input waveguide and symmetrical about only one plane, strong coupling into the  $TE_{11}$  and  $TM_{11}$  modes is almost unavoidable at frequencies close to their common cutoff frequency. As a result, the  $TE_{11}$  and  $TM_{11}$  cutoff frequency may be taken as the upper frequency limit of such a design. Because coupling to the higher modes falls off very quickly below the cutoff frequency, the OMT can operate quite close to this limit with little degradation in performance. The lower frequency limit is given by the cutoff frequency of the  $TE_{01}$  mode. This would give a maximum bandwidth of 1.41:1. However, it is difficult to achieve an acceptable return loss close to the  $TE_{01}$  cutoff due to the rapid variation in guide wavelength. A bandwidth of  $\sim 1.3:1$  is therefore a practical limit for such a design.

Manuscript received 19 April 2009.

A. Dunning is with the CSIRO Australia Telescope National Facility, Epping NSW Australia 1710.

S. Srikanth and A. R. Kerr are with the National Radio Astronomy Observatory, Charlottesville, VA 22903. Corresponding author: [akerr@nrao.edu](mailto:akerr@nrao.edu).

The National Radio Astronomy Observatory is a facility of the National Science Foundation operated under cooperative agreement by Associated Universities, Inc.

## II. A SPLIT-BLOCK OMT

The OMT described here consists of an input section, a polarization separating junction, and an output section for each polarization. The structure of the waveguide is shown in Fig. 1. The input section is composed of a square input which is reduced to a smaller square waveguide, followed by a transition to a waveguide with a T-shaped cross section. The polarization separating junction removes one polarization via a mitered bend and allows the other to pass through. Finally each output section consists of a stepped transition to a larger rectangular waveguide. The OMT was designed in three stages beginning with the junction of the dual-mode waveguide with two rectangular waveguides. Then the transition between the T-waveguide and the square waveguide was designed, and finally the input and output transitions were added.

The internal geometry of the polarization separating junction is shown in Fig. 2. Using a T-shaped waveguide makes it possible to maintain only two propagating modes within the 1.3:1 frequency band and simultaneously achieve a waveguide

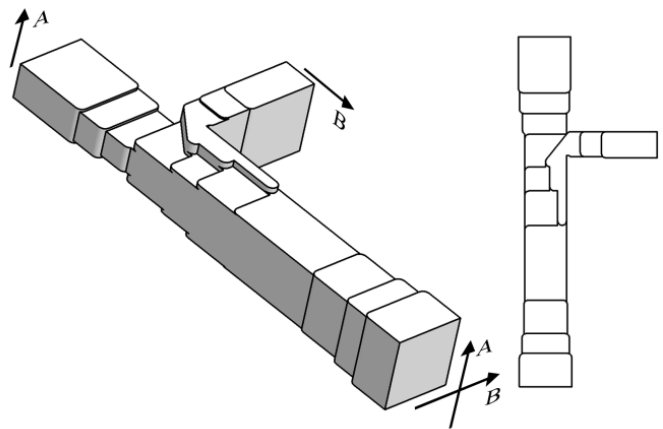


Fig. 1. Geometry of the OMT

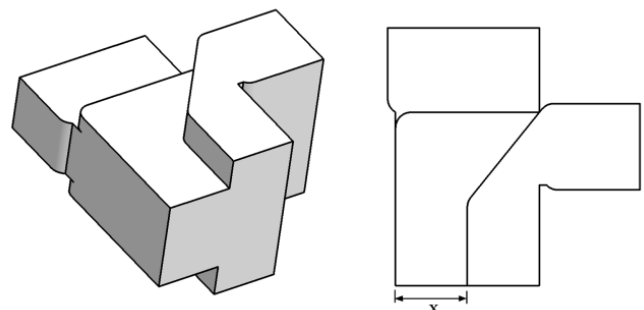


Fig. 2. Internal geometry of the polarization separating junction with the T-waveguide input.

impedance closely matched to that of the junction's rectangular waveguide outputs. The ratio of the cutoff frequency of the desired modes in the T-waveguide to the cutoff frequency of the next higher order mode is 1.73:1, which makes it possible for this junction to operate over a bandwidth of approximately 1.6:1. It is only the transition from square to T-waveguide that reduces this bandwidth to 1.3:1. The dominant modes in T-waveguide and their corresponding polarizations are shown in Fig. 3. The **A** polarization encounters a transition to rectangular waveguide via a linear increase in the narrow section of the T-waveguide (dimension  $x$  in Fig. 2.) until only a rectangular section remains. This transition presents a section of reduced impedance waveguide almost a quarter wavelength long that is compensated by reducing the impedance of the output waveguide. The **B** polarization is removed via a mitered bend through a rectangular waveguide at right angles to the T-waveguide. A small capacitive transverse ridge at the junction of the rectangular waveguide with the T-waveguide was found to improve the return loss of this polarization. Using a finite element electromagnetic simulator [7] all internal dimensions of the junction and the rectangular waveguide outputs were optimized for minimum reflection of the input signals.

The transition between the T-shaped waveguide and square waveguide consists of a two stage stepped transition. This transition was initially optimized alone and then in combination with the junction for optimal return loss in each polarization.

As a final step, quarter-wave transformers were added to the input and each output waveguide to transform to the required external waveguide sizes. The external square waveguide propagates four modes within the frequency band and therefore the smaller square waveguide section must be maintained for a significant distance from the junction to prevent generation of higher-order modes. Finally, the whole structure was optimized

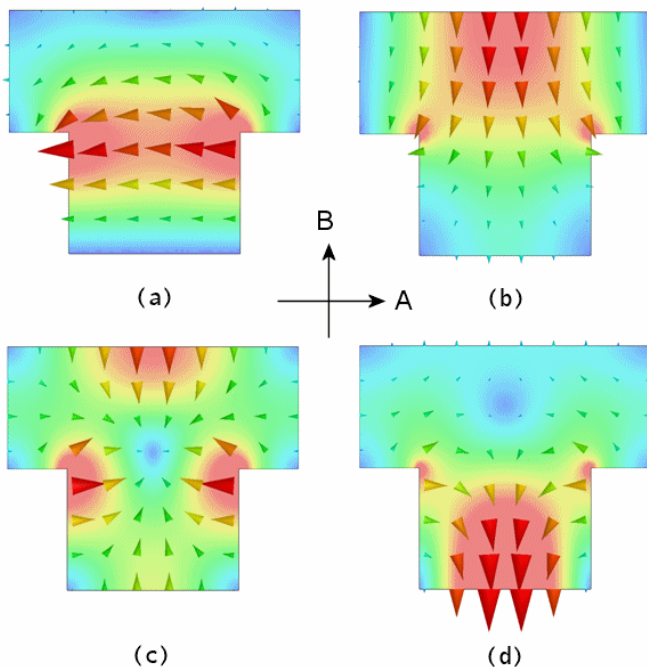


Fig. 3. Electric field of the first four modes of the T-waveguide. a) The mode corresponding to the  $TE_{01}$  mode in the square waveguide and the **A** polarization. b) The mode corresponding to the  $TE_{10}$  mode in the square waveguide and the **B** polarization. c) and d) show the next higher TM and TE modes, respectively.

for maximum return loss in both polarizations simultaneously.

The original design was for ALMA Band 6 (211-275 GHz) but for ease of measurement we constructed and measured a scaled version for 78-102 GHz in WR-10 waveguide as shown in Figs. 4 and 5.

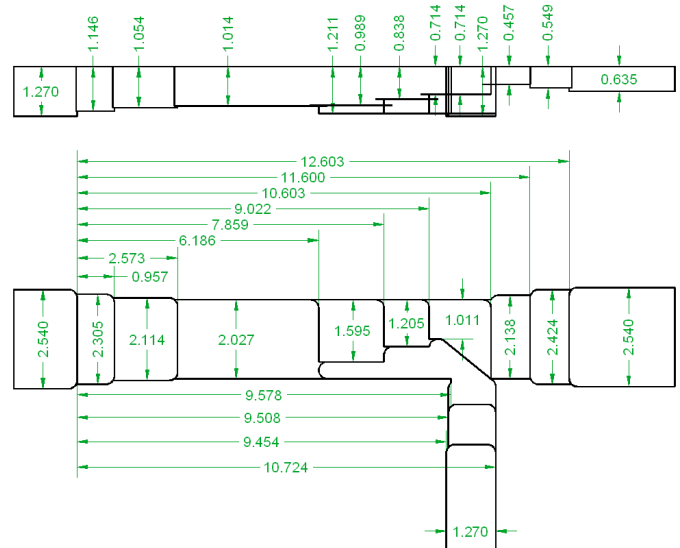


Fig. 4. Dimensions of the WR-10 OMT in mm. All corner radii are 0.216 mm.



Fig. 5. Photograph of the WR-10 OMT.

### III. SIMULATION AND MEASUREMENTS

The OMT was analyzed using the FDTD electromagnetic simulator QuickWave [8]. Fig. 6(a) shows the simulated transmission and reflection of the through and side paths (in Fig. 1, paths **A** and **B**, respectively).

Measurements were made using an HP8510C two port vector network analyzer with a square-to-rectangular waveguide transition on the square port of the OMT and a matched load on the rectangular port not connected to the VNA. Fig. 6(b) shows the measured transmission and reflection. The measured transmission shown in Fig. 6(b) has been corrected for the small loss of the square-to-rectangular transition.

Fig. 7 shows the polarization isolation measured with the VNA connected to the square port of the OMT and the isolated rectangular waveguide port.

The first OMT we made had poor polarization isolation as a result of misalignment between the block halves. To explore this, FDTD simulations were run with deliberately misaligned parts. Fig. 8 shows the effect of misalignments of 7, 14, and 28  $\mu\text{m}$  on the polarization isolation.

#### IV. DISCUSSION

The surprising sensitivity of the isolation of the OMT to small misalignments between block halves warrants further

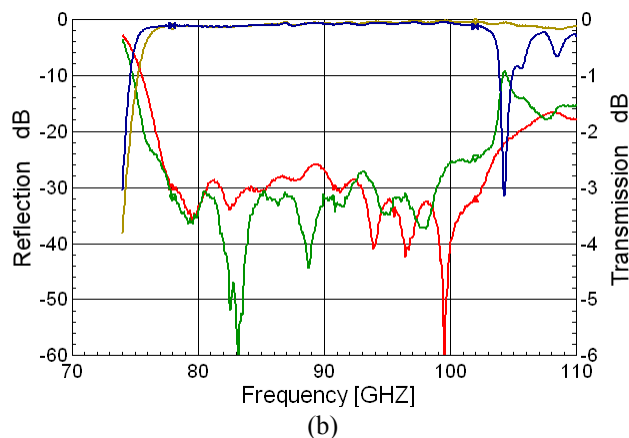
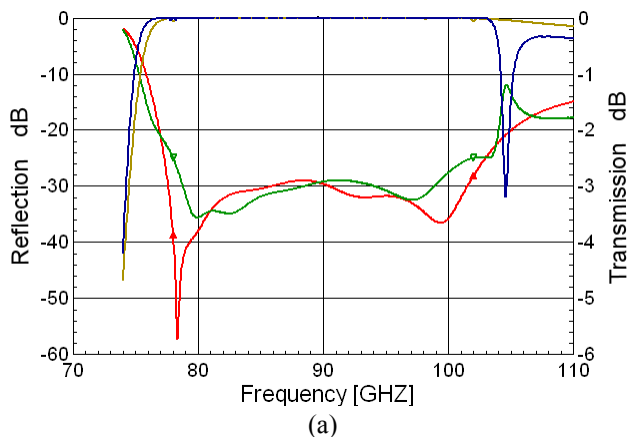


Fig. 6. S-parameters of the OMT: Transmission (side path blue, through path brown), and reflection coefficient (side arm green, through arm red) at the rectangular waveguide ports. (a) Simulated using QuickWave. (b) Measured. Markers at 78 and 102 GHz.

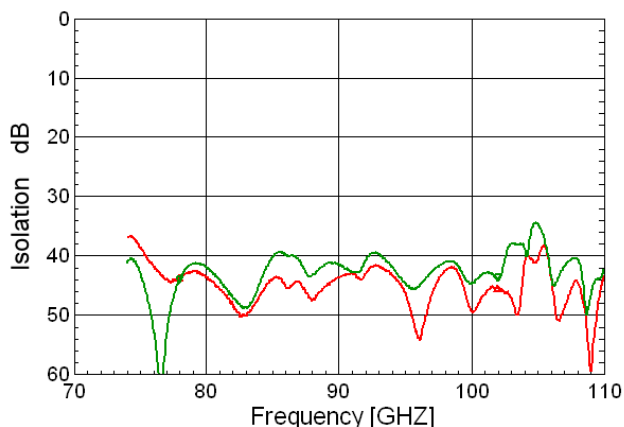


Fig. 7. Measured isolation of the OMT. Side-port isolation (red); through-port isolation (green). Markers at 78 and 102 GHz.

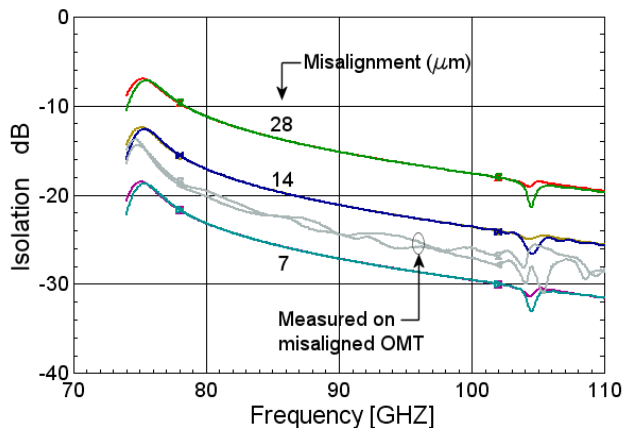


Fig. 8. Simulated polarization isolation as a function of misalignment between the block halves, for the side-port and through-port. Shown in gray are measurements on a misaligned OMT. Markers are at 78 and 102 GHz.

explanation. If the misalignment were simply equivalent to a twist in the square waveguide, the cross polarization would be much less than observed (and simulated). A 28  $\mu\text{m}$  misalignment of a 2.54 mm square waveguide would cause a rotation of  $\sim 0.3^\circ$ , corresponding to a -45 dB cross-polarized component independent of frequency. The actual cause of the frequency dependent cross-polarization can be explained with the aid of Fig. 9 which shows the misaligned square waveguide. Vector  $\mathbf{A}$  represents the electric field of one incident linear polarization, and can be broken down into two components  $\mathbf{A}_1$  and  $\mathbf{A}_2$ . Because of the misalignment of the two halves of the block, the two components see waveguides of slightly different effective width and thus have different phase velocities. This results in the

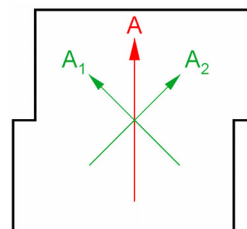


Fig. 9. Cross-section of the misaligned square waveguide. Components  $\mathbf{A}_1$  and  $\mathbf{A}_2$  of linearly polarized wave  $\mathbf{A}$  have different phase velocities which results in generation of a cross polarized component.

generation of circular polarization. At lower frequencies, close to the cutoff frequencies of the  $\mathbf{A}_1$  and  $\mathbf{A}_2$  modes, the difference in phase velocity is more pronounced, leading to the frequency dependence of the isolation shown in Fig. 8.

In principle the OMT can be scaled to operate at any frequency. In practice, scaling to higher frequencies will be limited by the precision of alignment between the block halves and by the ability to machine the small channels of the T-waveguide section. The smallest commercially available end-mills have a diameter of  $\sim 25 \mu\text{m}$  [9][10], which would allow an OMT to be machined for operation at 1300-1700 GHz. However, the best machining techniques would only permit alignment of the upper and lower parts within perhaps 2  $\mu\text{m}$ . This would give  $\sim 15$  dB isolation at the low end of the band in an OMT scaled for operation at 540-700 GHz.

It is interesting to speculate that in future receivers, in which the signal is digitized at the front end, it may be possible to correct the imperfect polarization isolation of an OMT digitally in the back end.

#### REFERENCES

- [1] A. M. Bøifot, E. Lier, and T. Schaug-Pettersen, "Simple and broadband orthomode transducer," Proc. Inst. Elect. Eng., vol. 137, no. 6, pt. H, pp. 396–400, Dec. 1990.
- [2] E. Wollack, "A Full Waveguide Band Orthomode Junction," Electronics Division Internal Report 303, National Radio Astronomy Observatory, May 1996. <http://www.gb.nrao.edu/electronics/edir/edir303.pdf>
- [3] E. J. Wollack and W. Grammer, "Symmetric waveguide orthomode junctions," Proc. ISSTT, pp. 169, 2003, and ALMA Memo 425, 2002. <http://www.alma.nrao.edu/memos/html-memos/alma425/memo425.pdf>
- [4] G. Narayanan and N. Erickson, "Full-Waveguide Band Orthomode Transducer for the 3 mm and 1 mm Bands," Proc. ISSTT, pp. 505-514, Mar 2002.
- [5] G. Moorey, R. Bolton, A. Dunning, R. Gough, H. Kanoniuk and L. Reilly, "A 77-117 GHz cryogenically cooled receiver for radioastronomy," Proc. Workshop on the Applications of Radio Science (WARS2006), Leura, NSW, Australia, 15-17 Feb. 2006.
- [6] A. Navarrini and R. Nesti, "Symmetric Reverse-Coupling Waveguide Orthomode Transducer for the 3-mm Band," IEEE Trans. Microwave Theory Tech. vol. 57, no. 1, pp. 80-88, Jan. 2009.
- [7] HFSS, Ansoft LLC, Pittsburgh PA. <http://www.ansoft.com/products/hf/hfss/>
- [8] QuickWave-3D, QWED Sp. z o.o., 02-010 Warsaw, Poland. [http://www.qwed.com.pl/qw\\_3d.html](http://www.qwed.com.pl/qw_3d.html)
- [9] Performance Micro Tool, Inc., Janesville, WI 53547. [http://www.pmtnow.com/end\\_mills/tools/TR-2.asp](http://www.pmtnow.com/end_mills/tools/TR-2.asp)
- [10] Harvey Tool Co., LLC., Rowley, MA 01969. <http://www.harveytool.com/products/>